Highly Efficient Inverted Phosphorescence OLEDs Based on Ultrathin Emitting Layer

Jun Liu, Xinkai Wu, Xingdong Shi, Jing Wang, Saijun Huang, Chaoping Chen, Jiangang Lu, Yikai Su and Gufeng He*

National Engineering Lab for TFT-LCD Materials and Technologies, and Department of Electronic Engineering, Shanghai Jiao Tong University, Shanghai 200240, People's Republic of China

Abstract

In this paper, we present highly efficient inverted phosphorescence organic light-emitting diodes (PhOLEDs) based on ultrathin emitting layers (EML). By introducing 1.5 nm EML with co-host, the inverted PhOLED exhibits external quantum efficiency (EQE) of 31.1%. Besides, a multilayer $mCP/MoO_3/Al/Cs_2CO_3$ works well as charge generation unit (CGU) for tandem inverted PhOLED with 0.5 nm EML.

1.   Introduction

Active-matrix organic light-emitting diodes (AMOLEDs) have been successfully commercialized in small and medium size and even flexible electronic products, such as smart phones, portable displays, and 3-dimensional TVs. In recent years, indium Gallium Zinc Oxide (IGZO)-thin film transistor (TFT) backplane for AMOLEDs has been attracted considerable attention to substitute for low temperature poly silicon (LTPS)-TFT backplane, since IGZO-TFT has advantages of uniformity large area and low cost.[1] Owing to the n-type nature of IGZO-TFT, inverted OLEDs with a bottom cathode are preferred to integrate with the IGZO-TFT for use in AMOLED.[2] Indium tin oxide (ITO) is commonly used as the cathode of inverted OLED due to its high optical transparency and electrical conductivity, but its high work function limits electron injection into the neighboring material with high lowest unoccupied molecular orbit (LUMO) level. A lot of electron injection layers (EILs), such as Mg, LiF, Cs_2CO_3, ZnO, and TiO_2, have been used for improved electron injection from ITO.[3-5] However, high performance inverted phosphorescence OLEDs (PhOLEDs) especially with external quantum efficiency (EQE) over 20% and low efficiency roll-off reported in conventional PhOLEDs are rare obtained. This is mainly because the ohmic contact at electrode/transporting layer interface and optimum charge balance within recombination zone with increasing current density are difficult to be achieved in the inverted structure. Among various methods proposed to improve the performance for PhOLEDs, host-guest doping remains the most effective strategy for all of today's state-of-the-art PhOLEDs. However, doping system requires complicated and time-consuming process for precise control of doping. To overcome the limitation, doping-free PhOLEDs provides a promising alternative while at risk of aggregation and self-quenching of common phosphorescent dyes with long lived triplets in the neat form. Recently, a bis[3,5-bis(2-pyridyl)-1,2,4-triazolato]platinum(II) $(Pt(ptp)_2)$ film with 100 nm thickness was selected as both electron transporting layer (ETL) and emitting layer (EML), and this doping-free PhOLED exhibited EQE of 20.3 ± 0.5%.[6] The short lifetime (469 ± 13 ns) of the $Pt(ptp)_2$ film is a key for the reduction of triplet quenching, and the electron-hole recombination was confined within a narrow region with 2 nm thickness near hole transporting layer (HTL)/$Pt(ptp)_2$ interface. On the other hand, ultrathin doping-free EML (less than 1 nm) of common phosphorescent dyes between HTL and ETL was introduced.[7] The ultrathin doping-free EML device demonstrated higher efficiency than the doped EML device, indicative of superior confinement of phosphor excited states in the ultrathin EML. However, recent reported EQE of PhOLED with doping system has exceeded 30% without outcoupling,[8,9] indicating non-optimized charge balance and self-quenching of phosphors in the doping-free EML device. Moreover, the doping-free system has not been used in inverted OLED structure.

Here, we present an inverted PhOLED based on an ultrathin (0.5 nm) doping-free EML consisted of phosphors with aggregation-induced phosphorescent emission (AIPE). The maximum EQE of 24.7%, and EQE of 20.9% at 1,000 cd/m^2 for the device are achieved. The surface morphology of EML was characterized by Atomic Force Microscopy (AFM). Accordingly, the ultrathin doping-free EML was simulated by a broadened thin (1.5 nm) doped EML with the same amount of phosphors. The device shows the maximum EQE of 31.1% and EQE of 24.2 % at 1,000 cd/m^2. Besides, tandem inverted PhOLED with a multilayer 1,3-bis(carbazol-9-yl)benzene (mCP)/MoO_3 (8 nm)/Al (1 nm)/Cs_2CO_3 (1 nm) as CGU shows almost twice voltage, CE and EQE than those of single unit device.

2.   Experimental

Figure 1 shows a schematic diagram of the inverted PhOLED structure and the chemical structure of the phosphorescent dye used in this study. The phosphorescent emitter is a bis-cyclometalated iridium complex of Ir(tfmppy)$_2$(tpip) (tfmppy = 4-trifluoromethylphenylpridine, tpip = tetraphenylimido-diphosphinate) featured with AIPE, which is a phenomenon showing weak phosphorescence in solution and enhanced phosphorescence emission in the solid state.[10] Cs_2CO_3 and MoO_3 are used as EIL and hole injection layer (HIL), respectively. 4,7-diphenyl-1,10-phenanthroline (Bphen) acts as ETL with high electron mobility. mCP and 1,3,5-tris (N-phenylbenzimidazole-2-yl)benzene (TPBI) are HTL and ETL, respectively. The inverted PhOLED was fabricated on patterned indium tin oxide (ITO)-coated glass substrates. Prior to film deposition, the ITO glass substrates were cleaned successively using deionized water, acetone and isopropanol ultrasonic bath, dried and then pretreated with oxygen plasma. The EIL, ETL, EML, HTL, HIL and anode Al were successively thermally deposited within a high vacuum deposition system at a base pressure of 10^{-6} torr. The deposition rate for organic materials was monitored by quartz-crystal monitors and kept constant within the range from 0.01 to 0.1 nm s^{-1}. For comparison, the conventional PhOLED with device structure of ITO/MoO_3 (6 nm)/mCP(49 nm)/Ir(tfmppy)$_2$(tpip) (0.5 nm)/TPBI (12.5 nm)/Bphen (35 nm)/Cs_2CO_3 (1 nm)/Al (100 nm) was fabricated. Additionally, the tandem inverted PhOLEDs with configuration of ITO/Cs_2CO_3 (1 nm)/Bphen (35 nm)/TPBI (12.5 nm)/Ir(tfmppy)$_2$(tpip) (0.5 nm)/mCP (49 nm)/MoO_3 (x nm)/Al (1 nm)/Cs_2CO_3 (1 nm)/Bphen (35 nm)/TPBI (12.5

nm)/Ir(tfmppy)$_2$(tpip) (0.5 nm)/mCP (49 nm)/MoO$_3$ (6 nm)/Al (85 nm) were also fabricated. Current density-voltage (J-V) and luminescence-voltage (L-V) characteristics were measured with a computer controlled Keithley 2400 source meter and BM-7A luminance colorimeter under ambient conditions. The surface morphologies of TPBI, Ir(tfmppy)$_2$(tpip) and mCP were measured by AFM.
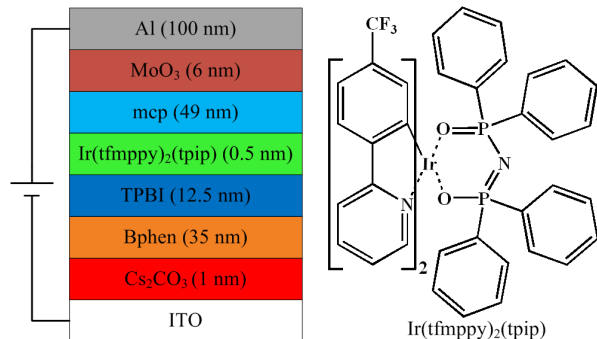

Figure 1. Schematic diagram of inverted PhOLED and chemical structure of the used phosphorescent dye.

3.   Results and discussion

Figure 2 shows energy level diagram of TPBI, Ir(tfmppy)$_2$(tpip) and mCP. Due to the large difference of the highest occupied molecular orbit (HOMO) energies of mCP and Ir(tfmppy)$_2$(tpip), holes are easily trapped by Ir(tfmppy)$_2$(tpip). Analogously, the high barrier of LUMO energies of TPBI and Ir(tfmppy)$_2$(tpip) facilitates electrons trapping by Ir(tfmppy)$_2$(tpip). Moreover, TPBI with high HOMO energy and mCP with low LUMO energy further favor confinement of holes and electrons to form recombination zone within the narrow EML.
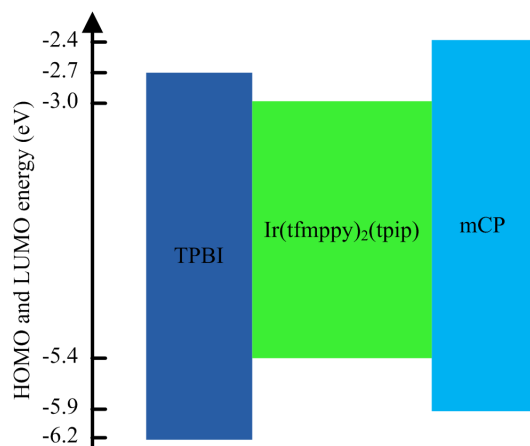

Figure 2. Energy level diagram of TPBI, Ir(tfmppy)$_2$(tpip) and mCP. Edges of rectangle correspond to HOMO (bottom) and LUMO (top) energies.

Figure 3 compares device performance of conventional and inverted PhOLED with ultrathin undoped EML. The inverted device consumes significantly increased voltage compared to the conventional device. For example, at current density of 1 mA/cm^2, driving voltage of the conventional device is about 3.8 V while that of the inverted device is about 6.8 V. Although Cs$_2$CO$_3$ and MoO$_3$ possess electron injection and hole injection ability, respectively, high work function of ITO leads to large electron injection barrier from ITO to Bphen and low work function of Al causes large hole injection barrier from Al to mCP. On the contrary, MoO$_3$ modified ITO and Cs$_2$CO$_3$ modified Al facilitate hole injection and electron injection for the conventional device, respectively. However, the inverted device shows remarkably enhanced EQE, indicating superior charge balance for the inverted device than that for the conventional device. This demonstrates that inferior charge injection at ITO/Cs$_2$CO$_3$ and Al/MoO$_3$ interfaces inversely prompts balance of holes and electrons in the inverted device. The maximum EQE, EQE at 1,000 cd/m^2 and at 10,000 cd/m^2 of the inverted device are 24.7%, 20.9% and 14.0%, respectively, while those of the conventional device are 13.3%, 13.0%, and 11.0%, indicative of larger efficiency roll-off in the inverted device. The efficiency roll-off in PhOLED is mainly associated with the factors such as triplet-triplet annihilation (TTA), triplet-polaron annihilation (TPA), loss of charge balance and field-induced exciton dissociation.[6] The low efficiency roll-off at the luminance ranging from 1,000 cd/m^2 to 10,000 cd/m^2 in the conventional device suggests that suppression of TTA and TPA processes, which are identically occurred in the inverted device. It is deduced that the large efficiency roll-off in the inverted device is mainly attributed to loss of charge balance and field-induced exciton dissociation. At small luminance, the inverted device achieves charge balance, resulting in high EQE. However, increasing driving voltage causes enhanced charge injection and break the charge balance, due to different dependence of hole and electron injection on the external electric field. On the other hand, the operation of the inverted device requires higher driving voltage, leading to higher electric field that will results in increased probability of exciton dissociation. Therefore, increased efficiency roll-off and decreased power efficiency are observed in the inverted device.

The phosphorescent dyes form a neat layer with 0.5 nm in view of device structure, however, their actual morphology on top of TPBI film should be measured by AFM. Figure 4 shows AFM images of (a) TPBI (10 nm) on the glass substrate, (b) Ir(tfmppy)$_2$(tpip) (0.5 nm) on the TPBI (10 nm), and (c) mCP (0.5 nm) on the TPBI (10 nm)/Ir(tfmppy)$_2$(tpip) (0.5 nm). The TPBI film surface exhibits a root mean square (RMS) roughness of 0.672 nm, indicating that the surface is not an absolute plane. This may be originated from the aggregation of TPBI molecules at the surface within a certain thickness. The deposition of Ir(tfmppy)$_2$(tpip) on TPBI occupies the concave and convex sites of TPBI surface, demonstrating that the Ir(tfmppy)$_2$(tpip) molecules are not in the form of neat layer but partially penetrate into TPBI. Next, the following deposition of mCP with 0.5 nm on the TPBI/Ir(tfmppy)$_2$(tpip) surface forms a homogeneous film with RMS roughness decreasing from 0.737 nm to 0.366 nm, referring that mCP molecules are prone to fill in the concave sites of TPBI/Ir(tfmppy)$_2$(tpip) surface. Therefore, Ir(tfmppy)$_2$(tpip) molecules with 0.5 nm thickness could be considered as guest partially doped into TPBI and mCP hosts. Accordingly, we fabricated another inverted PhOLED with structure of ITO/Cs$_2$CO$_3$ (1 nm)/Bphen (35 nm)/TPBI (12 nm)/TPBI:mCP:Ir(tfmppy)$_2$(tpip) (1:1:1, 1.5 nm)/mCP (48.5 nm)/MoO$_3$ (6 nm)/Al (100 nm) to simulate the ultrathin undoped EML structure. Since the amount of Ir(tfmppy)$_2$(tpip) is identical to that in the undoped EML, the device with host-guest system is denoted as the inverted doped EML device with equal guest amount. Such device shows increased voltage at current density larger than 1 mA/cm^2, compared to the inverted undoped EML device. In the doped EML, contact of mCP with electron blocking property and TPBI with hole blocking property is closer than that

in the undoped EML, which is responsible for the observed electrical curves. As co-host further facilitates hole and electron balance in the recombination zone, the equal doped EML device shows significantly enhanced EQE. The device achieves the maximum EQE of 31.1% and an EQE of 24.2% at the luminance of 1,000 cd/m^2. Recently, the conventional PhOLED without outcoupling was reported to have EQE over 30% due to the horizontal orientation of phosphorescent molecules within the co-host. The ultrahigh EQE of our device may be relevant to the molecule orientation of Ir(tfmppy)$_2$(tpip) in the co-host. To the best of our knowledge, the EQEs of device are among the best ever reported for an inverted PhOLED. Unfortunately, the inverted doped EML device has also large efficiency roll-off that is comparable to the inverted undoped EML device.
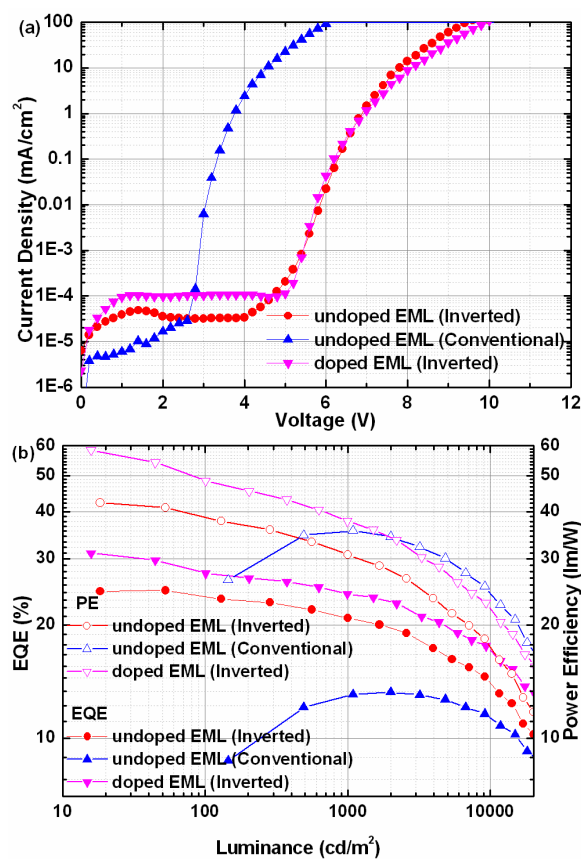

Figure 3. (a) Current density-voltage, and (b) EQE-power efficiency-luminance characteristics of conventional and inverted undoped EML and inverted doped EML PhOLEDs.

For the n-type IGZO-TFT AMOLED display, the combination of inverted tandem white OLEDs (WOLEDs)[11] and color filter is a promising proposal. The inverted tandem WOLED connecting two compensatory colors or three primary colors units with charge generation unit (CGU) shows enhanced efficiency and lifetime of device. The development of the inverted tandem WOLED should be based on the research of the inverted tandem OLED with single

color. Among various CGUs, MoO$_3$/HTL heterojunction and HTL doped by MoO$_3$ bulk heterojunction are the promising charge generation reservoirs,[12] due to charge transfer from the HOMO of HTL to the gap states of MoO$_3$. The HTL is not limited to triphenylamine based materials with low HOMO energy like N,N'-diphenyl-N,N'-bis(1-naphthyl)-1,1'-biphenyl-4,4''-diamine (NPB) and di-[4-(N,N-ditolyl-amino)-phenyl]cyclohexane (TAPC). Carbazole-based material with high HOMO energy such as 4,4'-bis(9-carbazolyl)biphenyl (CBP) was also reported to have charge transfer with MoO$_3$. However, MoO$_3$/mCP has not been reported in CGU. Here, we introduce mCP/MoO$_3$/Al/Cs$_2$CO$_3$ as CGU in the inverted tandem PhOLED, where Al/Cs$_2$CO$_3$ acts as electron injection layer. The tandem device structure is referred in the experimental section.
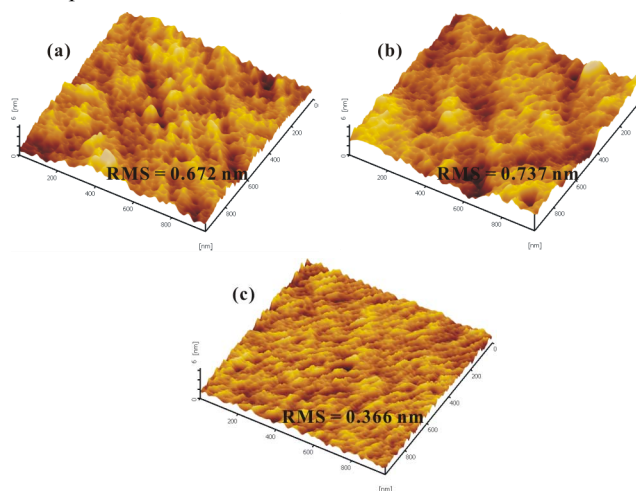

Figure 4. AFM images of (a) TPBI (10 nm) on the glass substrate, (b) Ir(tfmppy)$_2$(tpip) (0.5 nm) on the TPBI (10 nm), and (c) mCP (0.5 nm) on the TPBI (10 nm)/Ir(tfmppy)$_2$(tpip) (0.5 nm).

Figure 5 shows the performance of single unit device and tandem devices with mCP/MoO$_3$ (x nm)/Al(1 nm)/Cs$_2$CO$_3$(1 nm) as CGUs. As the thickness of MoO$_3$ film varies from 2 nm to 8 nm, MoO$_3$ film becomes homogeneous and continuous, the tandem devices exhibit gradually reduced driving voltage while increased CE and EQE. With mCP/MoO$_3$ (8 nm)/Al(1 nm)/Cs$_2$CO$_3$(1 nm) as CGU, at the luminance of 1,000 cd/m^2, the driving voltage (14.1 V) of tandem device is almost twice than that (7.0 V) of single unit device, and CE and EQE of tandem device are almost twice than those of single device, indicating that mCP/MoO$_3$ (8 nm)/Al(1 nm)/Cs$_2$CO$_3$(1 nm) works well as CGU for the inverted tandem PhOLED. The working mechanism of the CGU is described as follows. Electron transfer occurs from the HOMO states of mCP to the gap states of MoO$_3$ due to their energy level alignment, leading to hole generated at the HOMO of mCP. Under an external electric field, electron is extracted by EIL Al/Cs$_2$CO$_3$ and then transports in the neighboring Bphen layer, while hole transport in the mCP layer.
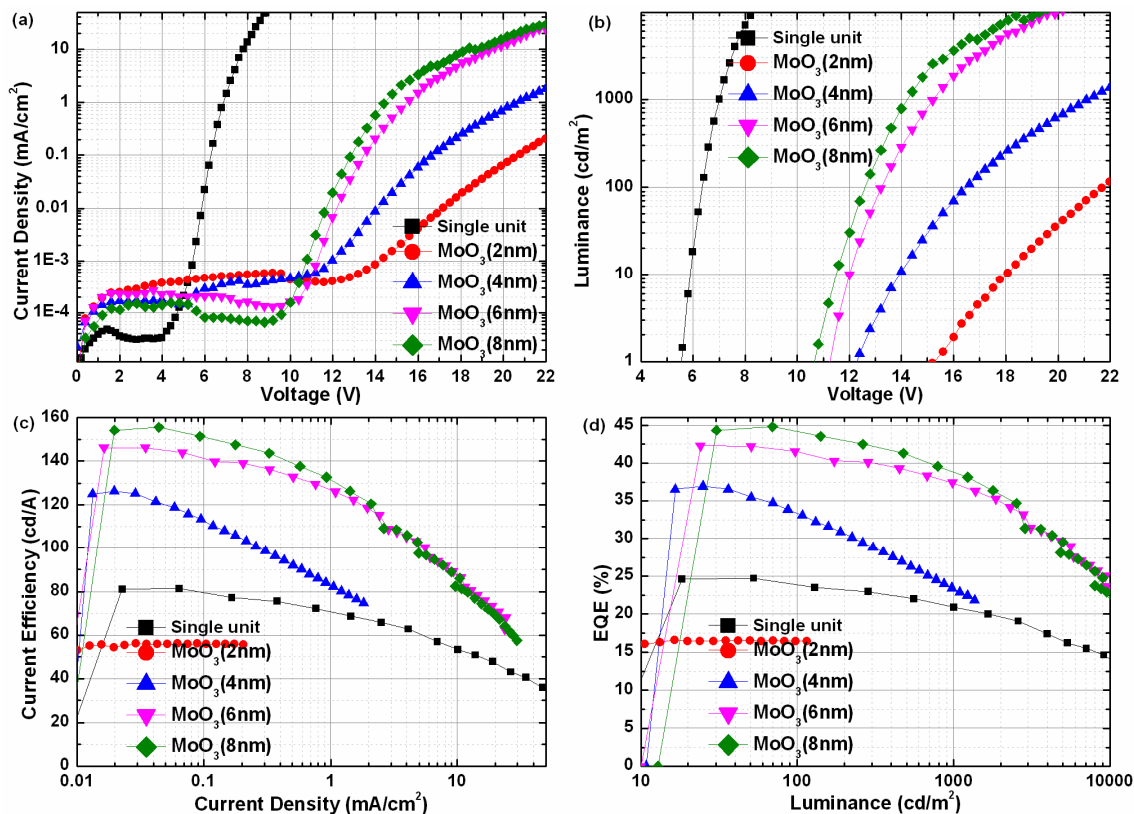
Figure 5. (a) Current density-voltage, (b) luminance-voltage, (c) current efficiency-current density, and (d) EQE-luminance characteristics of inverted tandem PhOLEDs with undoped EMLs.

4.   Summary

In summary, we report high efficiency inverted PhOLEDs based on ultrathin EML. By introducing phosphorescent dyes with AIPE as doping-free EML, the inverted PhOLED with 0.5 nm EML exhibits the maximum EQE of 24.7%, and an EQE of 20.9% at 1,000 cd/m^2. According to the surface morphology of undoped EML by AFM, the inverted PhOLED with 1.5 nm equal doped EML were fabricated. The maximum EQE of 31.1% and an EQE of 24.2 % at 1,000 cd/m^2 were achieved. These results are among the best ever reported in the literature for the inverted PhOLED. Additionally, tandem inverted PhOLED using mCP/MoO$_3$ (8 nm)/Al (1 nm)/Cs$_2$CO$_3$ (1 nm) as CGU shows almost twice current efficiency and EQE as those of single unit device. We believe that the inverted PhOLED based on ultrathin EML structure integrating readily with the n channel of IGZO-TFT backplane will promote large-size AMOLED display development.

5.   Acknowledgements

6.   References

[1] K. Nomura, H. Ohta, A. Takagi, T. Kamiya, M. Hirano, and H. Hosono, Nature 432, p. 488 (2004).

[2] T.-Y. Chu, J.-F. Chen, S.-Y. Chen, C.-J. Chen, and C. H. Chen, Appl. Phys. Lett. 89, p. 053503 (2006).

[3] T.-Y. Chu, J.-F. Chen, and C. H. Chen, Jpn. J. Appl. Phys. 45, p. 4948 (2006).

[4] T. Xiong, F. Wang, X. Qiao, and D. Ma, Appl. Phys. Lett. 89, p. 053518 (2006).

[5] H. Lee, C.-M. Kang, M. Park, J. Kwak, and C. Lee, ACS Appl. Mater. Interfaces 5, p. 1977 (2013).

[6] Q. Wang, I. W. H. Qswald, M. R. Perez, H. Jia, B. E. Gnade, and M. A. Qmary, Adv. Funct. Mater. 23, p. 5420 (2013).

[7] Y. Zhao, J. Chen, and D. Ma, ACS Appl. Mater. Interfaces 5, p. 965 (2013).

[8] S.-Y. Kim, W.-I. Jeong, C. Mayr, Y.-S. Park, K.-H. Kim, J.-J. Lee, C.-K. Moon, W. Brütting, and J.-J. Kim, Adv. Funct. Mater. 23, p. 3896 (2013).

[9] C. W. Lee, and J. Y. Lee, Adv. Mater. 25, p. 5365 (2013).

[10] Y.-C. Zhu, L. Zhou, H.-Y. Li, Q.-L. Xu, M.-T. Teng, Y.-X. Zheng, J.-L. Zuo, H.-J. Zhang, and X.-Z. You, Adv. Mater. 23, p. 4041 (2011).

[11] J. Liu, X. Shi, J. Wang, X. Wu, S. Huang, Z. Ye, J. Lu, Y. Su, G. He, and C. H. Chen, SID Digest p.1403 (2013).

[12] J.-P. Yang, Y. Xiao, Y.-H. Deng, S. Duhm, N. Ueno, S.-T. Lee, Y.-Q. Li, and J.-X. Tang, Adv. Funct. Mater. 22, p. 600 (2012).